

1 **Curcumin and turmeric extract inhibit SARS-CoV-2 pseudovirus cell entry and spike-**
2 **mediated cell fusion**

3

4 Authors: Endah Puji Septisetyani^{a*}, Dinda Lestari^{a,b}, Komang Alit Paramitasari^a, Pekik Wiji
5 Prasetyaningrum^a, Ria Fajarwati Kastian^a, Khairul Anam^c, Adi Santoso^a, Kartini Eriani^b

6

7 Authors Affiliation:

8 ^aMammalian Cell Engineering Research Group, Research Center for Genetic Engineering,
9 National Research and Innovation Agency (BRIN), Jl. Raya Bogor KM. 46, Cibinong,
10 Bogor, West Java, 16911, Indonesia

11 ^bUniversitas Syiah Kuala, Faculty of Mathematics and Natural Sciences, Department of
12 Biology, Banda Aceh, Indonesia

13 ^cResearch Center for Applied Microbiology, National Research and Innovation Agency
14 (BRIN), Jl. Raya Bogor KM. 46, Cibinong, Bogor, West Java, 16911, Indonesia

15

16 *Corresponding Author:

17 Name : Dr. Endah Puji Septisetyani, M.Sc.

18 Address: Research Center for Genetic Engineering, National Research and Innovation
19 Agency, Gedung Admin OR Hayati dan Lingkungan, BRIN, Jl. Raya Bogor KM 46,
20 Cibinong, Bogor, 16911, Indonesia

21 email: enda041@brin.go.id

22

23

24

25 **AUTHORS' CONTRIBUTION**

26 Conceptualization: Septisetyani EP. Data curation: Lestari D, Prasetyaningrum PW,
27 Paramitasari KA, Kastian RF, Septisetyani EP. Writing - original draft: Septisetyani EP,
28 Lestari D, Paramitasari KA. Writing - review & editing: Septisetyani EP, Prasetyaningrum
29 PW, Anam K, Santoso A., Eriani K.

30

31

32

33

34

35

36

37

38

39

40

41

42

43

44

45

46 **Curcumin and turmeric extract inhibit SARS-CoV-2 pseudovirus cell entry and spike-**
47 **mediated cell fusion**

48

49 Turmeric extract (TE) with curcumin as its main active ingredient has been studied as a
50 potential COVID-19 therapeutic. Curcumin has been studied in silico and in vitro against a
51 naive SARS-CoV-2 virus, yet little is known about TE's impact on SARS-CoV-2 infection.
52 Moreover, no study reveals the potential of both curcumin and TE on the inhibition of SARS-
53 CoV-2 cell-to-cell transmission. Here, we investigated the effects of both curcumin and TE on
54 inhibiting SARS-CoV-2 entry and cell-to-cell transmission using pseudovirus (PSV) and
55 syncytia models. We performed a PSV entry assay in 293T or 293 cells expressing hACE2.
56 The cells were pretreated with curcumin or TE and then treated with PSV with or without the
57 test samples. Next, we carried out syncytia assay by co-transfecting 293T cells with plasmids
58 encoding spike, hACE2, and TMPRSS2 to be treated with the test samples. The results showed
59 that in PSV entry assay on 293T/hACE/TMPRSS2 cells, both curcumin and TE inhibited PSV
60 entry at concentrations of 1 μ M and 10 μ M for curcumin and 1 μ g/ml and 10 μ g/ml for TE.
61 Moreover, both curcumin and TE reduced syncytia formation compared to control cells. Our
62 study shows that TE and curcumin are potential inhibitors of SARS-CoV-2 infection at entry
63 points, either by direct or indirect infection models.

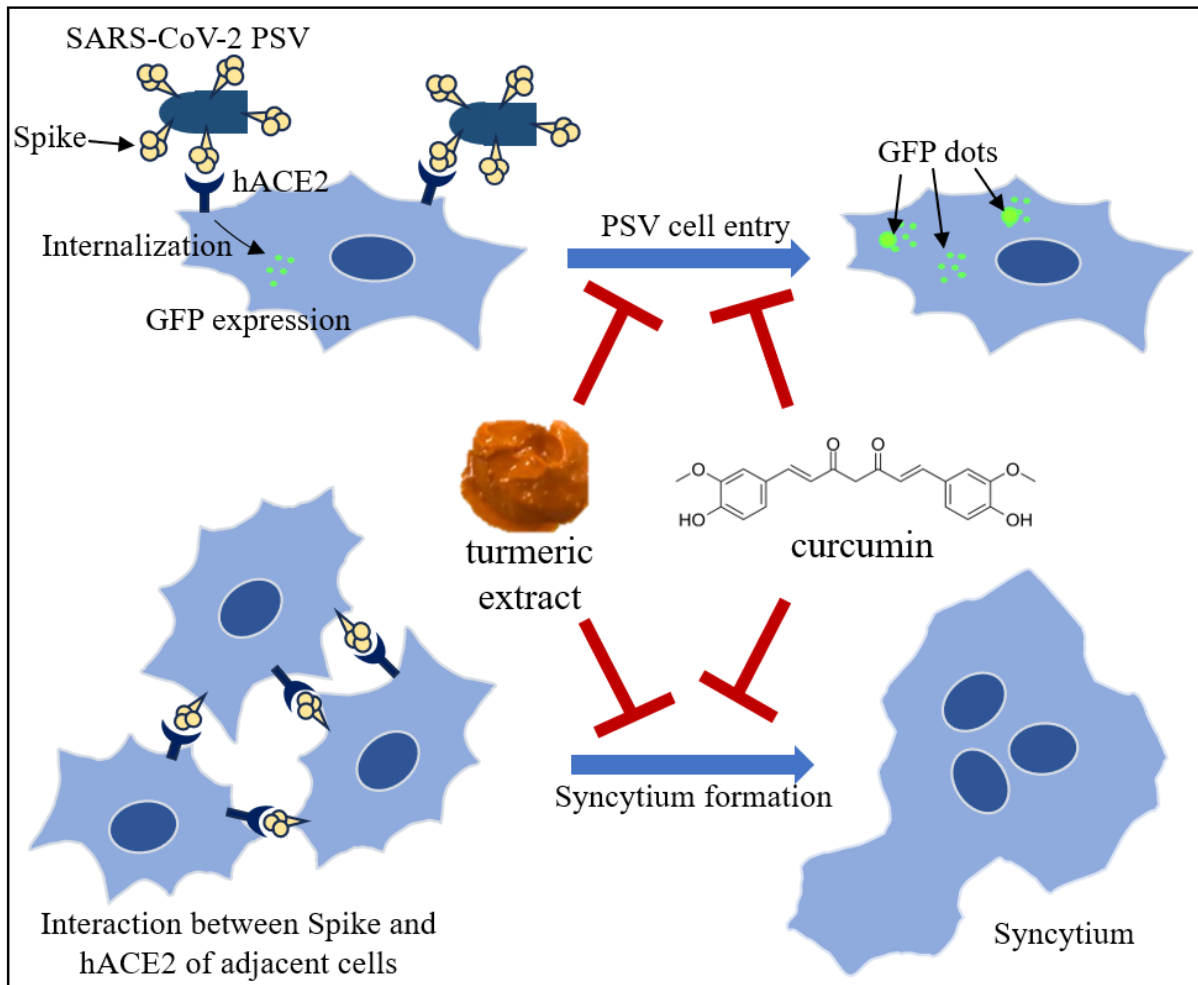
64 **Keywords:** COVID-19, curcumin, pseudovirus, SARS-CoV-2, syncytia, turmeric extract.

65

66

67

68 **GRAPHICAL ABSTRACT:**



69

70

71

72

73

74

75

76

77

78 1. INTRODUCTION

79 SARS-CoV-2 can infect the target cells by direct viral infection and cell-to-cell
80 transmission.^{1,2)} The first mode of viral infection has been widely explored by studying cell
81 and organ tropisms. SARS-CoV-2 infection toward various cell types has been performed,
82 which includes studies using pulmonary cancer cells Calu-3, kidney cells 293FT, liver cells
83 Huh7, colon cancer cells CaCO2, and Vero.^{3,4,5)} In addition, organ tropisms have been studied
84 using post-mortem tissue samples from COVID-19 patients and organoid models.⁶⁾ Based on
85 these studies, SARS-CoV-2 tropisms are strongly related to hACE2 expression as its target
86 receptor and TMPRSS2 protease, which enhances the viral entry process. SARS-CoV-2
87 infection involves the interaction of spike glycoprotein with hACE2, with or without spike
88 priming by TMPRSS2, to facilitate cell entry through endocytosis or membrane fusion
89 mechanisms.^{1,7)}

90 In addition, SARS-CoV-2 can be transmitted through a cell-to-cell mechanism, which
91 induces cell-to-cell fusion and syncytia formation.⁸⁾ Syncytia has been found in the lungs of
92 patients infected with SARS-CoV-2.⁹⁾ SARS-CoV-2 infection induces spike glycoprotein
93 expression. Eventually, as a transmembrane protein, spike protein will be transported to the
94 plasma membrane with the receptor binding domain (RBD) at the extracellular position, ready
95 for receptor binding. Similar to the virally integrated spike as the outer protein, cellular spike
96 protein can also bind to the adjacent cells' hACE2 receptor, which further induces cell-to-cell
97 fusion and finally forms a multinucleated giant cell or syncytium.^{8,9)} Syncytia formation has
98 been implicated with the severity of COVID-19 prognosis by several mechanisms, including
99 immune cell phagocytosis, antibody evasion, and induction of syncytial cell death.¹⁰⁾

100 Due to the availability of registered COVID-19 drugs and the continuous emergence of
101 daily COVID-19 cases, alternative treatments that can be easier to obtain for preventing and

102 treating future COVID-19 cases are essential to be developed. Turmeric (*Curcuma longa* L.) is
103 a WHO-selected medicinal plant growing in tropical areas.¹¹⁾ Turmeric rhizome has been
104 processed into turmeric decoction and turmeric extract, and some have been developed as a
105 standardized medicinal extract. Turmeric extract contains curcuminoid active compounds, with
106 curcumin as its main component.¹²⁾ Compared to the control group, Clinical studies have
107 demonstrated the effect of nano-encapsulated curcumin in reducing clinical manifestations of
108 COVID-19, such as fever, cough, and dyspnea.^{13,14)}

109 In silico analysis showed that curcumin has a high affinity for binding to the spike
110 glycoprotein through the formation of six hydrogen bonds,¹⁵⁾ thus, curcumin has the potential
111 to prevent the binding of the viral spike protein to the ACE2 receptor and inhibit the initiation
112 of the host cell infection process. Moreover, curcumin forms four hydrophobic interactions via
113 hydrogen bonds with TMPRSS2, which may inhibit cellular entry through the cell fusion
114 mechanism.¹⁶⁾

115 A plaque assay study in Vero cells has shown that curcumin inhibits SARS-CoV-2
116 infection in pre- and post-treatment of the D614 strain and Delta variant.¹⁷⁾ A study by Bormann
117 *et al.* shows that turmeric root juice and curcumin showed inhibition of SARS-CoV-2 infection
118 in Vero and Calu-3 cells determined by plaque assay and in-cell ELISA to detect the signal of
119 SARS-CoV-2 nucleocapsid protein (N).¹⁸⁾ Nonetheless, the effect of turmeric extract (TE) on
120 SARS-CoV-2 infection is less studied than curcumin. Moreover, there is no report about the
121 effects of both curcumin and TE on SARS-CoV-2 cell-to-cell transmission. In the present
122 study, we examined the effects of TE and curcumin on inhibiting SARS-CoV-2 infection using
123 the pseudovirus (PSV) and syncytia models for targeting viral entry points and cell-to-cell
124 transmission.

125

126 **2. MATERIALS AND METHODS**

127 **2.1. Cell culture and reagents**

128 The 293T (ECACC 12022001), CHO-K1 (ECACC 85051005), and 293 (ECACC 85120602)
129 cell lines are collections of the Research Center for Genetic Engineering, National Research
130 and Innovation Agency (BRIN, Indonesia). 293T cells were cultured in High-Glucose
131 Dulbecco's-modified Eagle's medium (Gibco, Billings USA) supplemented with 10% (v/v) of
132 heat-inactivated fetal bovine serum (Sigma-Aldrich, St. Louis USA) and antibiotics (100 µg/ml
133 streptomycin and 100 U/ml penicillin). CHO-K1 cells were cultured in F-12 medium (Sigma-
134 Aldrich, St. Louis USA) supplemented with 10% (v/v) of heat-inactivated fetal bovine serum
135 and antibiotics (100 µg/ml streptomycin and 100 U/ml penicillin). 293 cells were cultured in
136 MEM medium (Sigma-Aldrich, St. Louis USA) supplemented with 10% (v/v) of heat-
137 inactivated fetal bovine serum, 1% NEAA (Gibco, Billings USA), and antibiotics (100 µg/ml
138 streptomycin and 100 U/ml penicillin). Cells were grown inside a 37 °C tissue culture incubator
139 at 5% CO₂. The pcDNA3.1-SARS2-Spike (a gift from Fang Li; Addgene plasmid #145032),¹⁹⁾
140 pcDNA3.1-hACE (a gift from Fang Li; Addgene plasmid #145033),¹⁹⁾ and TMPRSS2 (a gift
141 from Roger Reeves; Addgene #53887) plasmids were obtained from Addgene.²⁰⁾ Cells were
142 transfected with expression vectors using polyethylenimine (PEI MAX® - Transfection Grade
143 Linear Polyethylenimine Hydrochloride (MW 40,000), Polysciences).

144 **2.2. Turmeric extract and curcumin preparation**

145 Turmeric extract (TE) was purchased as soft capsules (Natural Sari Kunyit, POM TR
146 192333771) from a GMP-certified manufacturer (PT. Industri Jamu dan Farmasi Sido Muncul
147 Tbk., Semarang, Indonesia). Each capsule was standardized to contain 350 mg of concentrated
148 liquid extract, equal to 100 mg of curcuminoids. The TE was dissolved in DMSO at 50 mg/mL,
149 and the stock was stored at -20 °C. The working solution was freshly prepared by serially
150 diluting the stock in culture media. Curcumin was obtained from Sigma (Cat. No. C1386-10G,

151 Lot#SLBD0850V) (Sigma-Aldrich, St. Louis, USA), reconstituted in DMSO at 50 mM, and
152 maintained as the stock at -20 °C. For every treatment involving curcumin, the working
153 solution was made at 10 and 100 µM concentrations by diluting the stock with complete culture
154 media with a maximum final concentration of DMSO less than 1%.

155 **2.3. MTT assay**

156 MTT cell viability assay was carried out in CHO-K1 and 293T cells. One day before the MTT
157 assay, 8×10^4 293T or 7×10^4 CHO-K1 cells per ml were seeded onto a 96-well plate. The next
158 day, the cells were treated and incubated with culture media containing various concentrations
159 of TE or curcumin for about 24 h. A set of wells containing cells without treatment and another
160 were prepared with medium only for background subtraction (blank). Following incubation,
161 the culture media containing TE or curcumin were discarded, and cells were washed with 1X
162 PBS. The cells were then incubated for 2 hours in 0.5 mg/mL MTT solution (3-(4,-5-
163 dimethylthiazo-2-yl)-2,5-diphenyltetrazolium bromide). At the end of incubation, MTT
164 reagents were discarded, and 100 µl of DMSO were added to each well and agitated at 100 rpm
165 for 10 minutes to ensure complete formazan crystals solubilization. Finally, the absorbance of
166 each well was recorded at 570 nm wavelength. Cell viability was calculated according to the
167 formula: $(OD_{\text{treated}} - OD_{\text{blank}}) / (OD_{\text{untreated}} - OD_{\text{blank}}) \times 100\%$

168 **2.4. Western blot**

169 Cell lysates were prepared using ice-cold RIPA buffer (Abcam, USA) with the addition of a
170 protease inhibitor cocktail. The total protein concentration was determined by BCA assay
171 (Thermo Scientific). About 10-40 µg protein was subjected to SDS-PAGE, and then the
172 resolved protein was transferred onto an activated PVDF membrane. The membrane was then
173 incubated in blocking buffer (5% skim milk in TBS/0.05% tween-20) followed by blotting with
174 primary antibodies (anti-SARS-CoV-2 spike (Abcam ab275759, USA) 1:2,000 or anti-β-actin
175 (Sigma A2228, USA) 1:4,000) for 2 h at room temperature or overnight at 4°C. After washing

176 with TBS/T, the membrane was incubated in secondary antibodies (ALP-conjugated antibodies
177 (Abcam ab6722), 1:4,000 or IR-Dye conjugated antibodies (LI-COR IRDye-680 RD),
178 1:10,000) in blocking buffer for about 2 h at room temperature or overnight at 4°C. Western
179 blot signal was detected by incubating the membrane with 1-StepTM NBT-BCIP substrate
180 solution (Thermo Scientific 34042) or observed by a LI-COR Odyssey CLx instrument.

181 **2.5. Immunofluorescence staining**

182 The 293T cells were seeded at a density of 3×10^4 cells/well on gelatin-coated cover glass placed
183 inside a 24-well plate. After about 3 h incubation, the cells were transfected overnight with the
184 pcDNA3.1-hACE2 expression vector. Transfected cells were washed with 1X PBS and fixed
185 with 4% paraformaldehyde for 10 min. Upon fixation, cells were permeabilized with 0.2 %
186 Triton-X, then incubated for 30 min at RT with blocking buffer (1% Bovine Serum Albumin
187 in 1X PBS) and further incubated for at least 1 hour at RT with rabbit anti-hACE2 antibody
188 (SAB 3500978, Sigma-Aldrich) or rabbit anti-TMPRSS2 antibody (BS-6285R, Bioss) diluted
189 in blocking buffer (1:250). Following primary antibody staining, cells were washed three times
190 with 1X PBS and incubated with goat anti-rabbit Alexa FluorTM 594 or 488 secondary antibody
191 (1:1,000) for 1 hour at RT. The secondary antibody was then washed with 1X PBS three times,
192 and the nuclei were stained with DAPI (4',6-diamidino-2-phenylindole)-containing mountant
193 (Abcam Ab104139). Samples were imaged with a motorized fluorescence microscope
194 (Olympus IX83, Tokyo, Japan).

195 **2.6. Preparation of SARS-CoV-2 pseudovirus**

196 Pseudotyping was performed in 293T cells transfected with a plasmid encoding SARS-CoV-2
197 spike (293T/spike). Briefly, 293T/spike cells were incubated at MOI ~3 for 1 h with
198 pseudotyped G*ΔG-GFP rVSV (Kerafast EH1024-PM).²¹⁾ Then, the medium was replaced
199 with a fresh medium containing anti-VSV-G antibody 1:2,000 to neutralize the excess of
200 G*ΔG-GFP rVSV and left overnight in the CO₂ incubator. A conditioned medium (CM)

201 containing pseudotyped spike*ΔG-GFP rVSV (SARS-CoV-2 pseudovirus) was collected and
202 spun the next day to remove cell debris. The supernatant was aliquoted and stored at -80° C
203 before being used for PSV entry assay.

204 **2.7. Pseudovirus entry assay**

205 PSV entry assay study was performed in the target cells of 293T transiently overexpressing
206 hACE2 and TMPRSS2 (293T/hACE2/TMPRSS2) or 293 cells stably expressing hACE2
207 (293/hACE2) prepared using lentivirus system. Briefly, 4×10^5 293T cells were grown in each
208 well of an 8-well chamber slide (SPL Life Sciences, Pyeongtaek, South Korea) previously
209 coated with 2% gelatin. Upon overnight incubation, the cells were transfected with vectors
210 harboring hACE2 and TMPRSS2 by using PEI. The next day, the medium was aspirated from
211 the cell monolayers, and cells were subjected to pretreatment with a complete medium
212 containing TE at 10 and 100 μg/ml or curcumin at 10 and 100 μM for 30 min. Then, the medium
213 was removed, and the PSV was added at 1:2 ratios in 300 μl of medium containing TE or
214 curcumin. After 16 h of viral infection, the cells were fixed and mounted. Finally, the images
215 of GFP dots that represented the internalization of pseudovirus were acquired using a motorized
216 fluorescence microscope (Olympus IX83). The GFP dots were counted from 8 different areas
217 and analyzed by Fiji software (National Institute of Health).

218 The 293/hACE2 stable cells were generated by transduction of 293 cells using
219 lentivirus produced in 293T cells utilizing plasmids: pCMV-dR8.2-dvpr (a gift from Bob
220 Weinberg; Addgene #8455);²²⁾ pCAGGS-G-Kan (Kerafast EH1017); and
221 RRL.sin.cPPT.SFFV/Ace2.IRES-neo.WPRE(MT129) (a gift from Caroline Goujon; Addgene
222 plasmid #145840).²³⁾ The 293/hACE2 population were then maintained in culture medium
223 containing G418 to obtain 293 cells that stably expressing recombinant hACE2. For the PSV
224 entry assay using 293/hACE2, the cells were grown onto gelatin-coated 8-chamber slides and

225 incubated overnight before PSV treatment. The GFP dots were counted from 5 different areas
226 and analyzed by Fiji software.

227 **2.8. Syncytia inhibition assay**

228 293T cells were seeded in a 24-well plate at 1.4×10^5 cells/ml density in DMEM supplemented
229 with 10% FBS. After overnight incubation, the cells were co-transfected with plasmids bearing
230 SARS-CoV-2 spike, hACE2, and TMPRSS2 and incubated for about 6 h. Subsequently, 500
231 μ l/well of dilutions of curcumin at 1 and 10 μ M or turmeric extract at 1 μ g/ml and 10 μ g/ml
232 was added to cell monolayers in duplicate and incubated for about 16 h. The following day,
233 syncytia formation was observed using an inverted microscope (Olympus CKX53), and 10
234 images were acquired to represent each well. The number of syncytia was calculated with Fiji
235 software and then sorted based on the number of nuclei using 4 categories: (i) <5 nuclei, (ii) 6-
236 10 nuclei, (iii) 11-15 nuclei, and (iv) >15 nuclei.

237 **2.9. Statistical analysis**

238 Data were presented as mean \pm SD (standard deviation) as indicated in each figure. Student's
239 t-test calculated statistical differences and a *p*-value <0.05 was considered significant.

240

241 **3. RESULTS**

242 **3.1. Cell viability assay of curcumin and TE on CHO-K1 and 293T cells**

243 Curcumin and TE have been known to show cytotoxic effects in various cancer cells, for
244 instance, breast cancer cells, colorectal cancer cells, and brain cancer cells.²⁴⁾ Also, even though
245 curcumin and TE show less cytotoxicity against normal cells at high concentrations, the toxic
246 effects could still be observed.²⁵⁾ Therefore, before we investigated their antiviral activities, we
247 evaluated the cytotoxicity of curcumin and TE on CHO-K1 and 293T cells to determine the
248 non-toxic concentration to be used in PSV entry and syncytia fusion assays.

249 We applied 1, 5, 10, 25, and 50 μM curcumin serial concentrations and 1, 5, 10, 25, and
250 50 $\mu\text{g/ml}$ TE for MTT assay in CHO-K1 cells. The results showed that after 24 hours of
251 curcumin treatment, the cell viability was 91.7, 96.09, 92.64, 39.06, and 35.19% as the
252 concentration increased (**Fig 1a**). In addition, after a 24-hour treatment, CHO-K1 cell viability
253 declined according to increased TE concentrations of 95.82, 91.08, 72.61, 41.66, and 26.27 %, ,
254 respectively (**Fig 1b**). Moreover, we tested the effect of curcumin and TE in 293T cells using
255 serial concentrations of 1, 10, and 100 μM curcumin or 1, 10, and 100 $\mu\text{g/ml}$ TE for 24 h. The
256 results indicated that the cell viability of 293T cells after curcumin treatment was 86.52, 74.18,
257 and 11.09 % (**Fig 1c**). In addition, the cell viability after TE treatment was 81.52, 76.54, and
258 5.33 %, respectively (**Fig 1d**). Higher concentrations of tested samples significantly reduced
259 cell viability, with the 293T cells showing more susceptibility to curcumin and TE treatment
260 than CHO-K1 cells. Therefore, to minimize the cytotoxic effect of tested samples in further
261 assays, we applied lower concentrations of curcumin (1 and 10 μM) and TE (1 and 10 $\mu\text{g/ml}$)
262 and treated the cells for only about 16-18 h.

263 **3.2. Pseudovirus entry assay**

264 We prepared SARS-CoV-2 PSV with a VSV backbone and GFP reporter in spike-
265 transfected 293T cells (pseudotyped spike* ΔG -GFP rVSV). Spike expression in 293T/spike
266 cells used for pseudotyping was confirmed by Western blot. Moreover, we also detected spike
267 in the CM obtained after pseudotyping, indicating the formation of SARS-CoV-2 pseudovirus
268 and its release into the culture medium (**Fig 2**).

269 Furthermore, we used the CM to perform a PSV entry assay in 293T overexpressing
270 hACE2/TMPRSS2 and 293/ACE2 stable cells. The 293T/hACE2/TMPRSS2 cells were
271 pretreated with curcumin or TE for 30 min, then treated with PSV/curcumin or PSV/TE,
272 followed by 16-18 h incubation in a CO_2 incubator. GFP expression indicating PSV

273 internalization and viral genome release was observed by fluorescence microscopy with 60x
274 magnification to expose the GFP dots (**Fig 3a**). To confirm that GFP dots were formed within
275 the cells, we also observed the cells in bright field mode and used DAPI to stain the nuclei. The
276 representative images are shown in **Fig 3b**. As the results showed, nontreated cells showed a
277 higher number of GFP dots compared to the treated cells with fluorescence focus units (FFU)
278 296 ± 2 . The FFU of cells treated with curcumin 1 and 10 μM were 141 ± 8.76 and 56 ± 6.52 .
279 Whereas FFU of cells treated with TE 1 and 10 $\mu\text{g/ml}$ were 81 ± 5.93 and 49 ± 3.31 . Cells treated
280 with curcumin and TE significantly reduced the FFU number, especially at higher
281 concentrations, indicating the potential inhibitory effect on SARS-CoV-2 viral cell entry (**Fig**
282 **3c**).

283 Next, we clarified the inhibitory effect of curcumin as the active compound to inhibit
284 SARS-CoV-2 PSV entry by performing an entry assay in 293 cells that stably expressed ACE2
285 (293/ACE2) (**Fig 4a**). Besides treating the 293/ACE2 cells with curcumin before PSV addition,
286 the curcumin was combined with PSV after incubation for 30 min (**Fig 4b**). The representative
287 images of cells after the PSV entry assay are shown in **Fig 4c**. As a quantification result, the
288 number of GFP dots/cell for non-treated cells was 1.45. The number of GFP dots per cell in
289 curcumin and PSV/curcumin-treated cells was 0.99, while the number of GFP dots per cell in
290 curcumin-treated cells was 0.887. The results indicated that curcumin reduced PSV entry,
291 especially for curcumin pretreatment before the addition of PSV ($P = 0.035$) (**Fig 4d**).

292 **3.3. Syncytia formation assay**

293 This assay represents the cells infected with SARS-CoV-2 and expressing its membrane
294 protein spike, which can bind the hACE2 receptor of the adjacent cell. Instead of using the
295 original virus, we transfected the cells directly with spike plasmid. We used 293T cells
296 transfected with plasmids encoding SARS-CoV-2 spike, hACE2, and TMPRSS2 to perform

297 the syncytia assay. The cells expressing spike will locate the Spike in the transmembrane
298 region, enabling the interaction between spike with the hACE2 receptor and TMPRSS2 of the
299 adjacent cells. As a result, the two interacting cells will form an intercellular bridge that
300 eventually will fuse and form multinucleated cells.²⁶⁾ The more cells interact and fuse, the more
301 multinucleated cells or syncytia will be generated, as shown in **Fig 5a**.

302 We show that 293T cells, after transfection and treatment with DMSO 0.1% and 1%,
303 formed syncytia as much as 31.4 and 15.75 per field. In addition, the treatment of cells with
304 curcumin and TE reduced the number of syncytia. The number of syncytia formed after cell
305 treatment with curcumin 1 and 10 μ M was 15.85 ($P<0.0001$ vs DMSO 0.1%) and 5.5
306 ($P<0.0001$ vs DMSO 1%), while the number of syncytia formed after cell treatment with TE 1
307 and 10 μ g/ml was 14.05 ($P<0.0001$ vs DMSO 0.1%) and 6.6 ($P<0.0001$ vs DMSO 0.1%) (**Fig**
308 **5b**).

309 Furthermore, we analyzed the distribution of nuclei numbers within the syncytia and
310 categorized them into <5 , 5-10, 11-15, and >15 . The syncytia with nuclei number <5 for DMSO
311 0.1, curcumin 1 μ M, and TE 1 μ g/ml were 3.65, 4.25, 2, while nuclei number 5-10 were 9.8,
312 4.5, 35.5, nuclei no 11-15 were 5.95, 3.3, 4.35, and nuclei number >15 were 11.75, 2.8, 4.25.
313 The syncytia with nuclei number <5 for DMSO 1, curcumin 10 μ M and TE 10 μ g/ml were 2,
314 2, 1.8, while nuclei number 5-10 were 6.05, 1.75, 2.3, nuclei no 11-15 were 3.85, 0.9, 1.85, and
315 nuclei no >15 were 3.85, 0.4, 0.85. These data indicated that treatment of the cells with
316 curcumin and TE reduced the nuclei number within syncytia, representing lower fusion events
317 than the DMSO treatment (**Fig 5c**).

318 **4. DISCUSSION**

319 Curcumin has been tested for its anti-SARS-CoV-2 activities by plaque assay in Vero
320 cells. Using the original virus, curcumin inhibits SARS-CoV-2 infection.¹⁷⁾ However, surface

321 receptors in Vero cells differ from human cells, and the study may not correlate well with actual
322 events.²⁷⁾ Thus, the antiviral study of curcumin has also been carried out using human Calu-3
323 cells, which endogenously express hACE2 and TMPRSS2. A study using these cells
324 demonstrated that curcumin may inhibit SARS-CoV-2 viral replication as indicated by reduced
325 N protein expression following viral infection.¹⁸⁾ Besides investigating curcumin's antiviral
326 effect, Bormann *et al.* also tested the effect of turmeric juice (water extract).¹⁸⁾ However, the
327 antiviral study of turmeric extract (TE) has not been widely reported compared to its active
328 compound, curcumin.

329 In this manuscript, we reported the SARS-CoV-2 antiviral activities of curcumin and
330 TE, especially at the entry point, using the pseudovirus and syncytia models to represent cell-
331 to-cell transmission. Here, we showed that curcumin and TE reduced PSV entry in
332 293T/hACE2/TMPRSS2 cells, in which 10 μ M curcumin and 10 μ g/ml TE significantly
333 affected the number of GFP dots. The effect of TE was comparable to the curcumin effect on
334 PSV cell entry in which 10 μ g/ml TE was equal to 2.86 μ g/ml curcuminoid, with the majority
335 of curcumin content and 10 μ M curcumin being equal to 3.68 μ g/ml of curcumin.

336 From the previous studies, Marin-Palma *et al.* reported that 10 μ M curcumin can inhibit
337 SARS-CoV-2 infection in Vero E6 cells.¹⁷⁾ It is also reported that curcumin inhibits SARS-
338 CoV-2 infection at concentrations of 3-10 μ M.²⁸⁾ Furthermore, in A549 cells, curcumin shows
339 SARS-CoV-2 antiviral concentration of 5 μ M.²⁹⁾ We also showed that curcumin inhibited PSV
340 entry in 293/hACE2 cells. These results corroborate curcumin effects against SARS-CoV-2
341 infection with our data representing curcumin inhibition at PSV cell entry point. It has been
342 known that curcumin affects the early stages of viral replication cycles, including viral-receptor
343 attachment, internalization, and fusion that have been studied against several types of viruses,
344 which involve influenza, dengue, zika, chikungunya, pseudorabies, and VSV.^{30,31,32)}

345 Moreover, curcumin and TE inhibit secondary infection via cell-to-cell transmission in
346 a syncytia formation model mediated by SARS-CoV-2 spike expression. Cells treated with
347 curcumin and TE showed smaller syncytia with fewer nuclei than control cells. The more cells
348 fused to generate syncytia, the larger syncytia with more nuclei will be formed, and vice versa.

349 Based on *in silico* data, curcumin can also interact with SARS-CoV-2 spike RBD,³³⁾
350 hACE2,³⁴⁾ and TMPRSS2.¹⁶⁾ These data align with our results that curcumin inhibited PSV
351 entry and syncytia formation. Our *in vitro* study using PSV and syncytia models revealed that
352 both curcumin and TE are potential inhibitors of SARS-CoV-2 infection, especially at the entry
353 points either by direct infection or cell-to-cell transmission mediated by spike-induced cell
354 fusion. Curcumin can interfere with the spike-receptor binding during direct viral or
355 intercellular transmission, hindering viral infection and cell fusion.¹⁷⁾ In addition, TE, as the
356 crude extract that contains curcumin, also has the potential to inhibit SARS-CoV-2 infection
357 and potentially to be developed as an independent herbal-derived product for the prevention of
358 viral infection with curcuminoids used as identity compounds for TE standardization.

359

360 **ACKNOWLEDGEMENTS**

361 We are grateful for the financial support from the Educational Fund Management
362 Institution/National Research and Innovation Agency (LPDP/BRIN) (grant no. 102/FI/P-
363 KCOVID-19.2B3/IX/2020 and RIIM No. KEP-5/LPDP/LPDP.4/2022) and Research
364 Organization for Life Sciences and Environment, BRIN (Research Program (DIPA Rumah
365 Program) 2022).

366

367 **CONFLICT OF INTEREST**

368 The authors declared no potential conflict of interest.

369

370 **REFERENCES**

- 371 1) Jackson CB, Farzan M, Chen B, Choe H. Mechanisms of SARS-CoV-2 entry into cells.
372 *Nat. Rev. Mol. Cell. Biol.*, **23**, 1–18 (2021).
- 373 2) Rajah MM, Hubert M, Bishop E, Saunders N, Robinot R, Grzelak L, Planas D, Dufloo
374 J, Gellenoncourt S, Bongers A, Zivaljic M, Planchais C, Guivel-Benhassine F, Porrot F,
375 Mouquet H, Chakrabarti LA, Buchrieser J, Schwartz O. SARS-CoV-2 Alpha, Beta, and
376 Delta variants display enhanced spike-mediated syncytia formation. *EMBO J.*, **40**,
377 e108944 (2021).
- 378 3) Hoffmann M, Kleine-Weber H, Schroeder S, Krüger N, Herrler T, Erichsen S, S,
379 Schiergens TS, Herrler G, Wu NH, Nitsche A, Müller MA, Drosten C, Pöhlmann. SARS-
380 CoV-2 cell entry depends on ACE2 and TMPRSS2 and is blocked by a clinically proven
381 protease inhibitor. *Cell*, **181**, 271-280 (2020).
- 382 4) Katopodis P, Randeva HS, Spandidos DA, Saravi S, Kyrou I, Karteris E. Host cell entry
383 mediators implicated in the cellular tropism of SARS-CoV-2, the pathophysiology of
384 COVID-19 and the identification of microRNAs that can modulate the expression of
385 these mediators (Review). *Int. J. Mol. Med.*, **49**, 20 (2022).
- 386 5) Saccon E, Chen X, Mikaeloff F, Rodriguez JE, Szekely L, Vinhas BS, Krishnan S,
387 Byrareddy SN, Frisan T, Végvári Á, Mirazimi A, Neogi U, Gupta S. Cell-type-resolved
388 quantitative proteomics map of interferon response against SARS-CoV-2. *iScience*, **24**,
389 102420 (2021).
- 390 6) Peng L, Gao L, Wu X, Fan Y, Liu M, Chen J, Song J, Kong J, Dong Y, Li B, Liu A, Bao
391 F. Lung organoids as model to study SARS-CoV-2 infection. *Cells*, **11**, 2758 (2022).

- 392 7) Hirano T, Murakami M. COVID-19: A new virus, but a familiar receptor and cytokine
393 release syndrome. *Immunity*, **52**, 731-733 (2020).
- 394 8) Zheng Y, Zhou LL, Su Y, Sun Q. Cell fusion in the pathogenesis of COVID-19. *Mil.*
395 *Med. Res.*, **8**, 68 (2021).
- 396 9) Lin L, Li Q, Wang Y, Shi Y. Syncytia formation during SARS-CoV-2 lung infection: a
397 disastrous unity to eliminate lymphocytes. *Cell Death Differ.*, **28**, 2019–2021, (2021).
- 398 10) Rajah MM, Bernier A, Buchrieser J, Schwartz O. The mechanism and consequences of
399 SARS-CoV-2 spike-mediated fusion and syncytia formation. *J. Mol. Biol.*, **434**, 167280
400 (2022).
- 401 11) World Health Organization. *Rhizoma Curcumae Longae. WHO monographs on selected*
402 *medicinal plants*. Vol. 1, WHO, Geneva, pp. 115-124 (1999).
- 403 12) Sharifi-Rad J, Rayess YE, Rizk AA, Sadaka C, Zgheib R, Zam W, Sestito S, Rapposelli
404 S, Neffe-Skocińska K, Zielińska D, Salehi B, Setzer WN, Dosoky NS, Taheri Y, El
405 Beyrouthy M, Martorell M, Ostrander EA, Suleria HAR, Cho WC, Maroyi A, Martins
406 N. Turmeric and its major compound curcumin on health: bioactive effects and safety
407 profiles for food, pharmaceutical, biotechnological and medicinal applications. *Front.*
408 *Pharmacol.*, **11**, 01021 (2020).
- 409 13) Tahmasebi S, El-Esawi MA, Mahmoud ZH, Timoshin A, Valizadeh H, Roshangar L,
410 Varshoch M, Vaez A, Aslani S, Navashenaq JG, Aghebati-Maleki L, Ahmadi M.
411 Immunomodulatory effects of nanocurcumin on Th17 cell responses in mild and severe
412 COVID-19 patients. *J. Cell Physiol.*, **236**, 5325–5338 (2021).
- 413 14) Valizadeh H, Abdolmohammadi-Vahid S, Danshina S, Ziya GM, Ammari A, Sadeghi A,
414 Roshangar L, Aslani S, Esmaeilzadeh A, Ghaebi M, Valizadeh S, Ahmadi M. Nano-
415 curcumin therapy, a promising method in modulating inflammatory cytokines in
416 COVID-19 patients. *Int. Immunopharmacol.*, **89**, 107088 (2020).

- 417 15) Maurya VK, Kumar S, Prasad AK, Bhatt MLB, Saxena SK. Structure-based drug
418 designing for potential antiviral activity of selected natural products from Ayurveda
419 against SARS-CoV-2 spike glycoprotein and its cellular receptor. *Virusdisease*, **31**, 179–
420 193 (2020).
- 421 16) Motohashi N, Vanam A, Gollapudi R. In silico study of curcumin and folic acid as potent
422 inhibitors of human transmembrane protease serine 2 in the treatment of COVID-19.
423 *INNOSC Theranostics and Pharmacological Sciences*, **16**, 3–9 (2020).
- 424 17) Marín-Palma D, Tabares-Guevara JH, Zapata-Cardona MI, Flórez-Álvarez L, Yepes
425 LM, Rugeles MT, Zapata-Builes W, Hernandez JC, Taborda NA. Curcumin inhibits in
426 vitro SARS-CoV-2 infection in Vero E6 cells through multiple antiviral mechanisms. *J.*
427 *Molecules*, **26**, 6900 (2021).
- 428 18) Bormann M, Alt M, Schipper L, van de Sand L, Le-Trilling VTK, Rink L, Heinen N,
429 Madel RJ, Otte M, Wuensch K, Heilingloh CS, Mueller T, Dittmer U, Elsner C, Pfaender
430 S, Trilling M, Witzke O, Krawczyk A. Turmeric root and its bioactive ingredient
431 curcumin effectively neutralize SARS-CoV-2 in vitro. *Viruses*, **13**,1914 (2021).
- 432 19) Shang J, Ye G, Shi K, Wan Y, Luo C, Aihara H, Geng Q, Auerbach A, Li F. Structural
433 basis of receptor recognition by SARS-CoV-2. *Nature*, **581**, 221-224 (2020).
- 434 20) Edie S, Zaghoul NA, Leitch CC, Klinedinst DK, Lebron J, Thole JF, McCallion AS,
435 Katsanis N, Reeves RH. Survey of human chromosome 21 gene expression effects on
436 early development in *Danio rerio*. *G3 (Bethesda)*, **8**, 2215-2223 (2018).
- 437 21) Whitt MA. Generation of VSV pseudotypes using recombinant Δ G-VSV for studies on
438 virus entry, identification of entry inhibitors, and immune responses to vaccines. *J. Virol.*
439 *Methods*, **169**, 365-374 (2010).

- 440 22) Stewart SA, Dykxhoorn DM, Palliser D, Mizuno H, Yu EY, An DS, Sabatini DM, Chen
441 IS, Hahn WC, Sharp PA, Weinberg RA, Novina CD. Lentivirus-delivered stable gene
442 silencing by RNAi in primary cells. *RNA*, **9**, 493-501 (2003).
- 443 23) Rebendenne A, Valadão ALC, Tauziet M, Maarifi G, Bonaventure B, McKellar J, Planès
444 R, Nisole S, Arnaud-Arnould M, Moncorgé O, Goujon C. SARS-CoV-2 triggers an
445 MDA-5-dependent interferon response which is unable to control replication in lung
446 epithelial cells. *J. Virol.*, **95**, e02415-20 (2021).
- 447 24) Tomeh MA, Hadianamrei R, Zhao X. A review of curcumin and its derivatives as
448 anticancer agents. *Int. J. Mol. Sci.*, **20**, 1033 (2019).
- 449 25) Li P, Pu S, Lin C, Liu H, Zhao H, Yang C, Guo Z, Xu S, Zhou Z. Curcumin selectively
450 induces colon cancer cell apoptosis and S cell cycle arrest by regulates Rb/E2F/p53
451 pathway. *J. Mol. Struct.*, **1263**, 133180 (2022).
- 452 26) Buchrieser J, Dufloo J, Hubert M, Monel B, Planas D, Rajah MM, Planchais C, Porrot
453 F, Guivel-Benhassine F, Van der Werf S, Casartelli N, Mouquet H, Bruel T, Schwartz
454 O. Syncytia formation by SARS-CoV-2-infected cells. *EMBO J.*, **39**, e106267 (2020).
- 455 27) Pandamooz S, Jurek B, Meinung CP, Baharvand Z, Sahebi Shahem-Abadi A, Haerteis
456 S, Miyan JA, Downing J, Dianatpour M, Borhani-Haghighi A, Salehi MS. Experimental
457 models of SARS-CoV-2 infection: possible platforms to study COVID-19 pathogenesis
458 and potential treatments. *Annu. Rev. Pharmacol. Toxicol.*, **62**, 25-53 (2022).
- 459 28) Wen CC, Kuo YH, Jan JT, Liang PH, Wang SY, Liu HG, Lee CK, Chang ST, Kuo CJ,
460 Lee SS, Hou CC, Hsiao PW, Chien SC, Shyur LF, Yang NS. Specific plant terpenoids
461 and lignoids possess potent antiviral activities against severe acute respiratory syndrome
462 coronavirus. *J. Med. Chem.*, **50**, 4087–4095 (2007).

- 463 29) Goc A, Sumera W, Rath M, Niedzwiecki A. Phenolic compounds disrupt spike-mediated
464 receptor-binding and entry of SARS-CoV-2 pseudo-virions. *PLoS ONE*, **16**, e0253489
465 (2021).
- 466 30) Mounce BC, Cesaro T, Carrau L, Vallet T, Vignuzzi M. Curcumin inhibits Zika and
467 chikungunya virus infection by inhibiting cell binding. *Antivir. Res.*, **142**, 148–57 (2017).
- 468 31) Chen DY, Shien JH, Tiley L, Chiou SS, Wang SY, Chang TJ, Lee YJ, Chan KW, Hsu
469 WL. Curcumin inhibits influenza virus infection and haemagglutination activity. *Food*
470 *Chem.*, **119**, 1346–1351 (2010).
- 471 32) Chen TY, Chen DY, Wen HW, Ou JL, Chiou SS, Chen JM, Wong ML, Hsu WL.
472 Inhibition of enveloped viruses infectivity by curcumin. *PLoS ONE*, **8**, e62482 (2013).
- 473 33) Shanmugarajan D, Prabitha P, Kumar BRP, Suresh B. Curcumin to inhibit binding of
474 spike glycoprotein to ACE2 receptors: computational modelling, simulations, and
475 ADMET studies to explore curcuminoids against novel SARS-CoV-2 targets. *RSC Adv.*,
476 **10**, 31385-31399 (2020).
- 477 34) Subbaiyan A, Ravichandran K, Singh SV, Sankar M, Thomas P, Dhama K, Malik YS,
478 Singh RK, Chaudhuri P. In silico molecular docking analysis targeting SARS-CoV-2
479 spike protein and selected herbal constituents. *J. Pure Appl. Microbiol.*, **14**, 989-998
480 (2020).
- 481
- 482
- 483
- 484
- 485
- 486

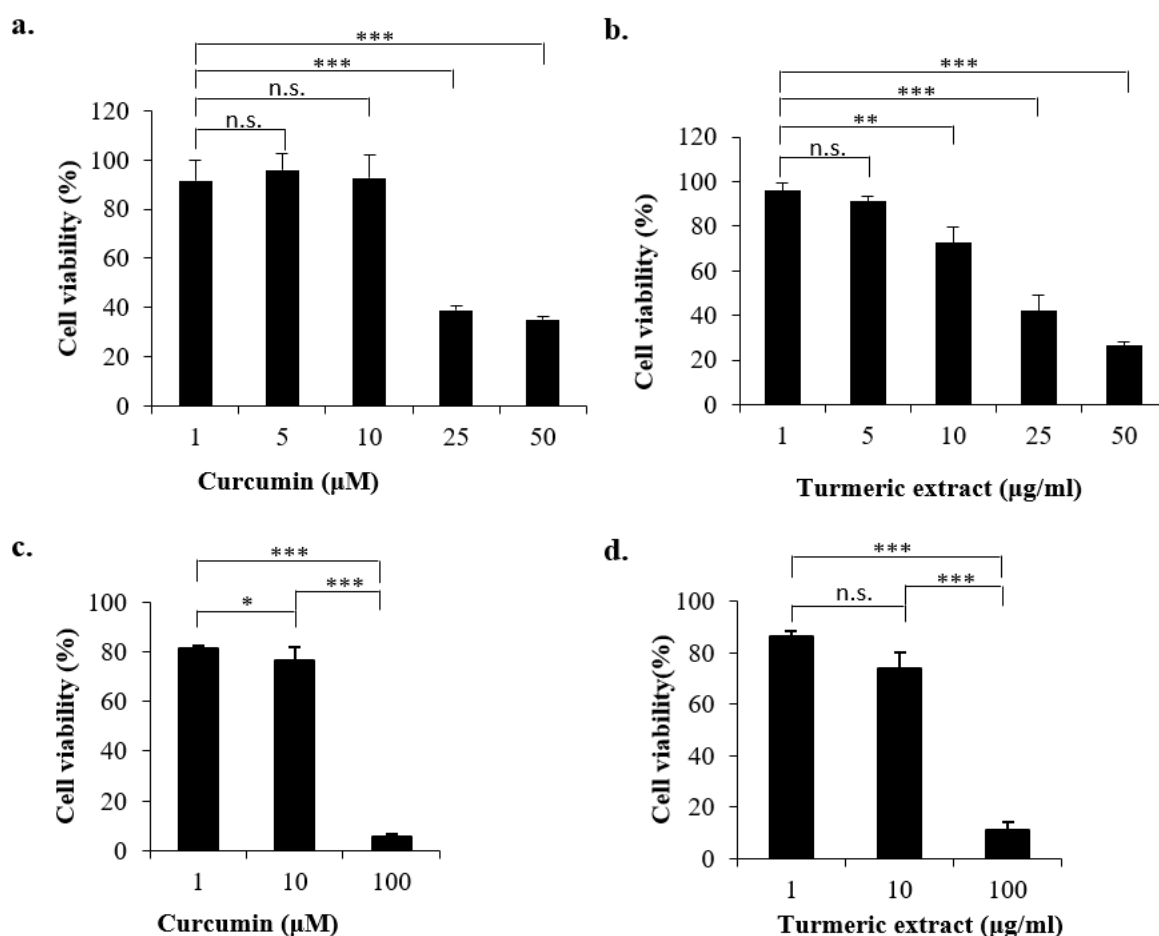
487

488

489

490

491 **FIGURE LEGENDS**



492

493 **Fig 1. CHO-K1 (a-b) cell viability profiles and 293T cells (c-d) after curcumin and**

494 **turmeric extract treatment.** Cells were plated onto a 96-well plate and treated with the tested

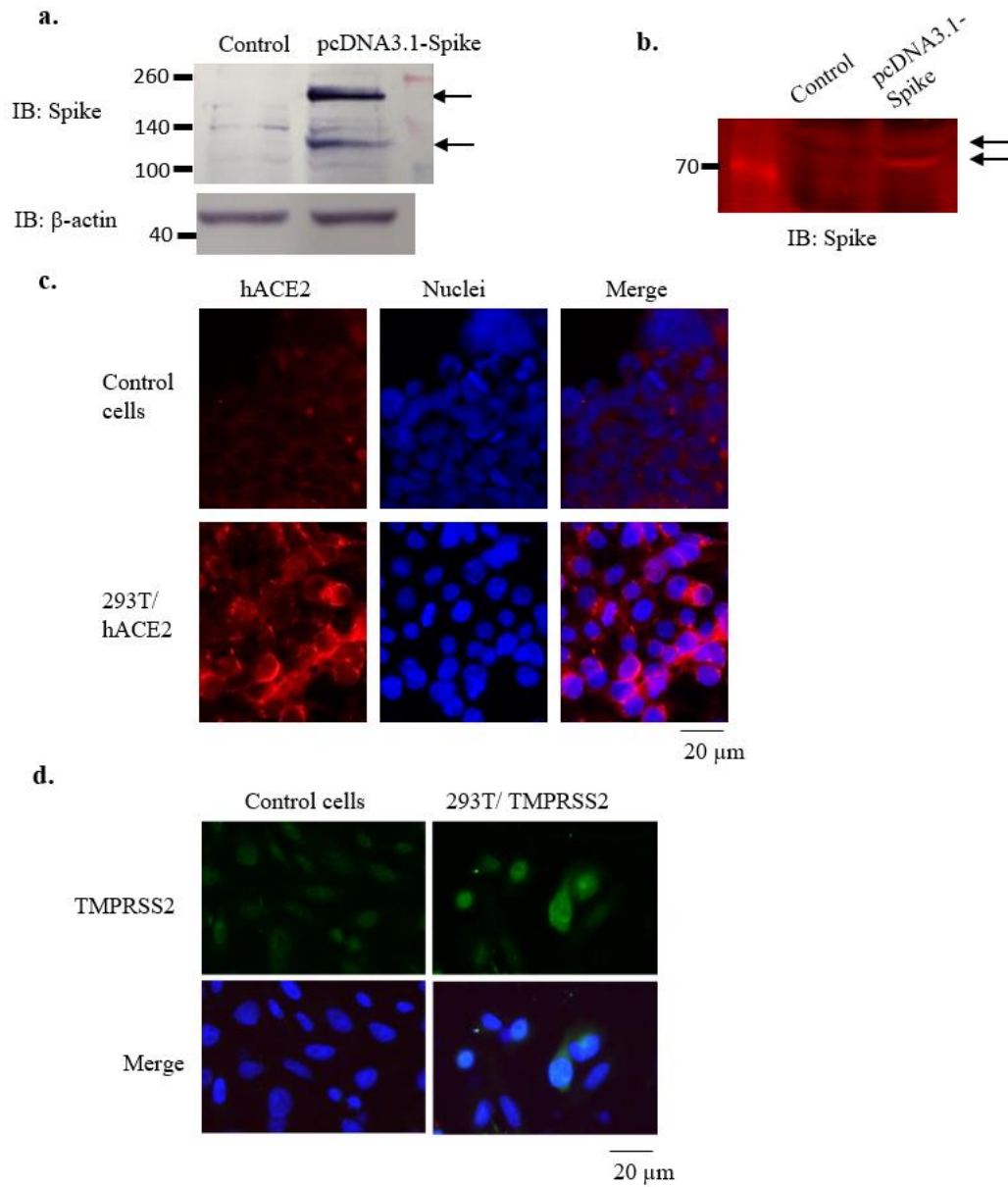
495 samples (n=3) for 24 h. The medium was then replaced with an MTT-containing medium and

496 incubated for 2 h. At the end of incubation, the formazan generated was dissolved with DMSO,

497 and the optical density was measured at 570 nm.

498

499



500

501 **Fig 2. Observation of spike, hACE2, and TMPRSS2 expression.** a. Detection of spike

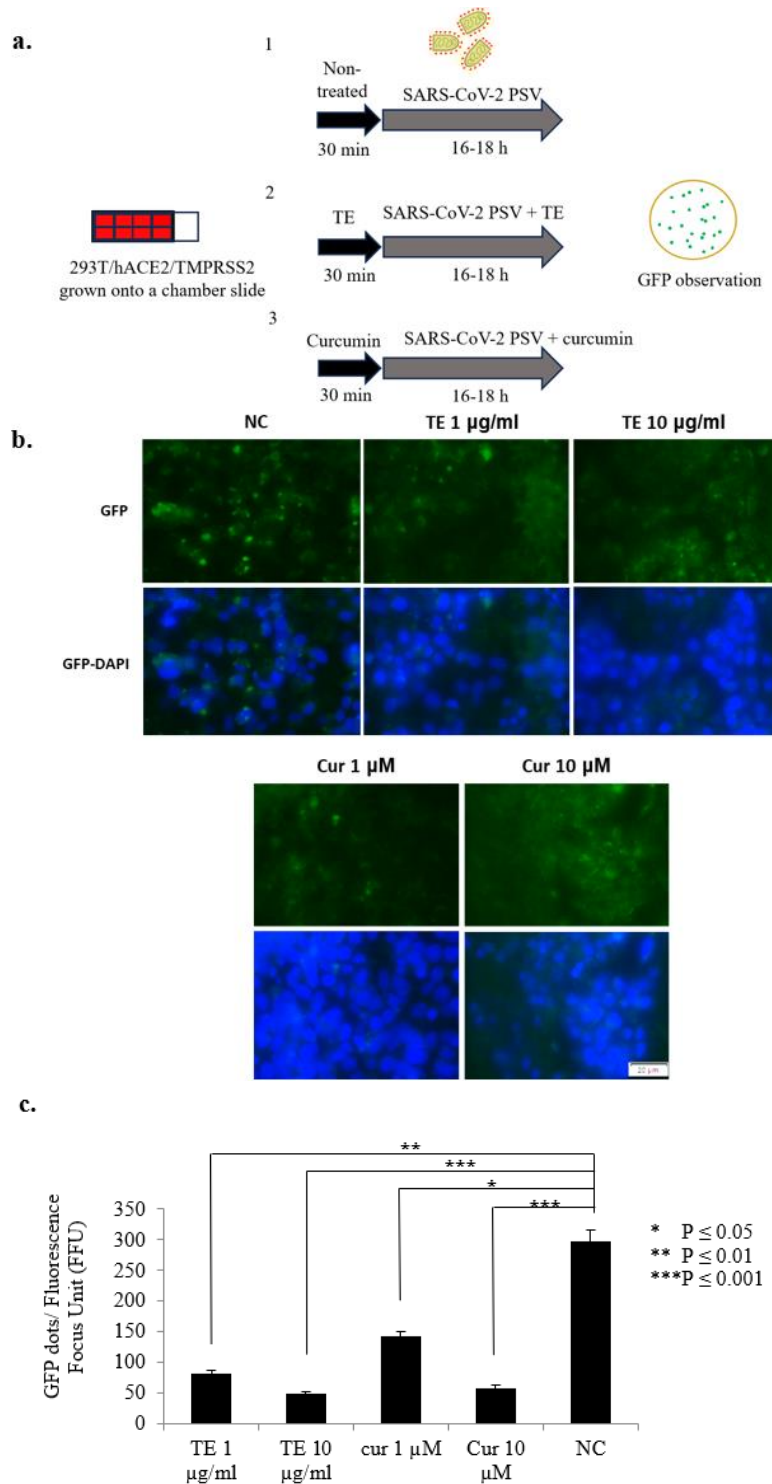
502 expression in 293T cells transfected with spike plasmid. b. Detection of spike in the

503 conditioned medium, which represented SARS-CoV-2 PSV. c-d. Detection of hACE2 and

504 TMPRSS2 expression by immunofluorescence staining.

505

506



507

508

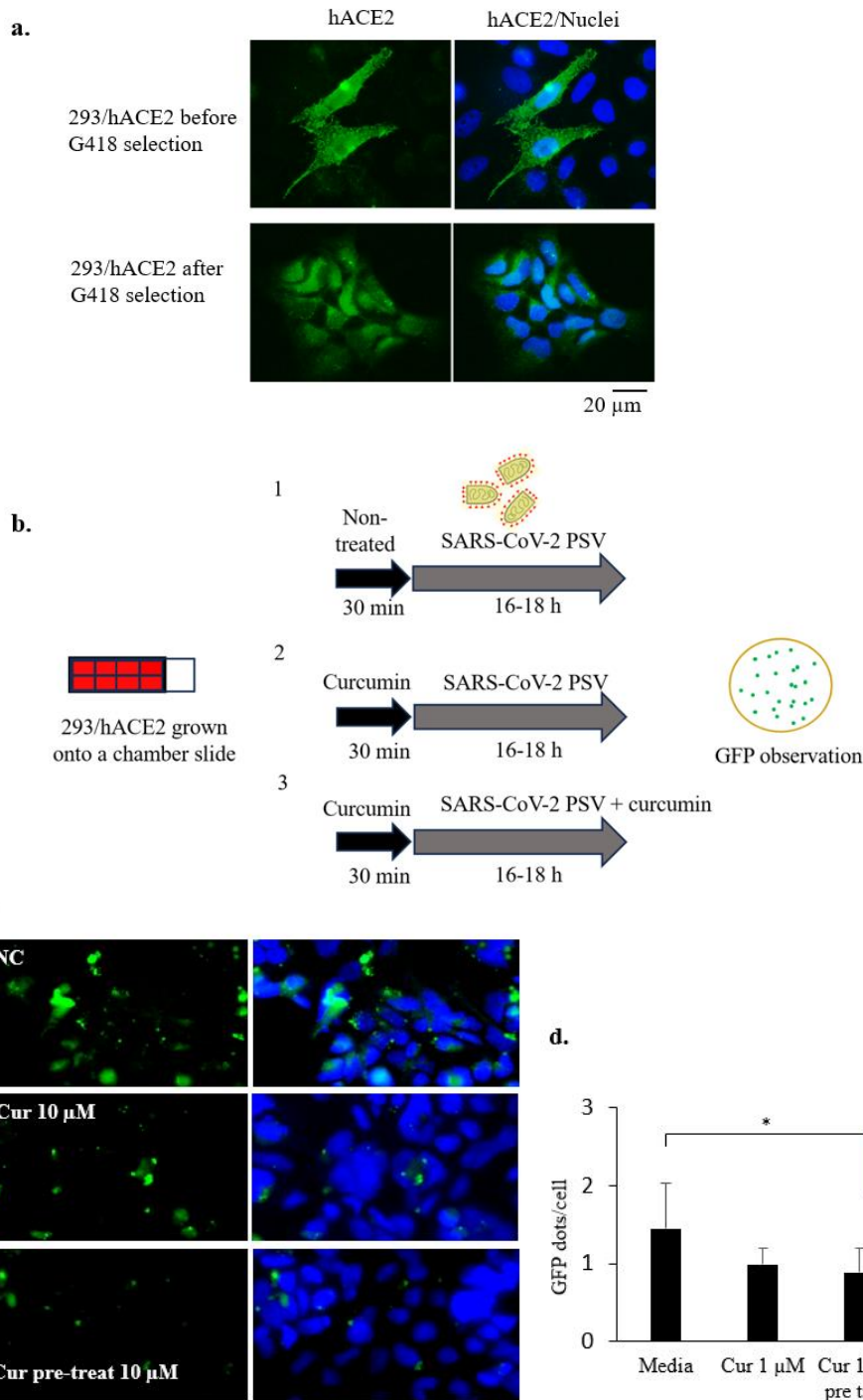
509 **Fig 3. Effect of turmeric extract and curcumin on PSV entry in 293T/hACE2/TMPRSS2**

510 **cells.** a. Schematic representation of PSV entry assay in 293T/hACE2/TMPRSS2 cells. b. The

511 representative image shows GFP dots to represent PSV internalization. c. Graph representing

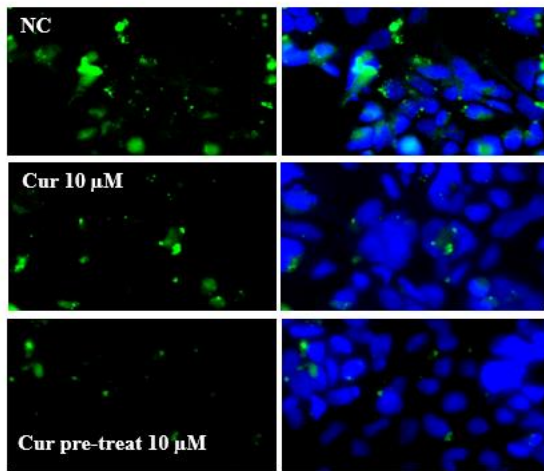
512 quantification of GFP dots (n = 8 microscope fields). TE: turmeric extract; Cur: curcumin; NC:

513 nontreated cells.

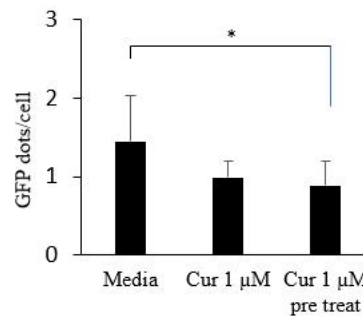


514

c.



d.



515

516 **Fig 4. Effect of curcumin on PSV entry in 293/ACE2 cells.** a. Observation of hACE2

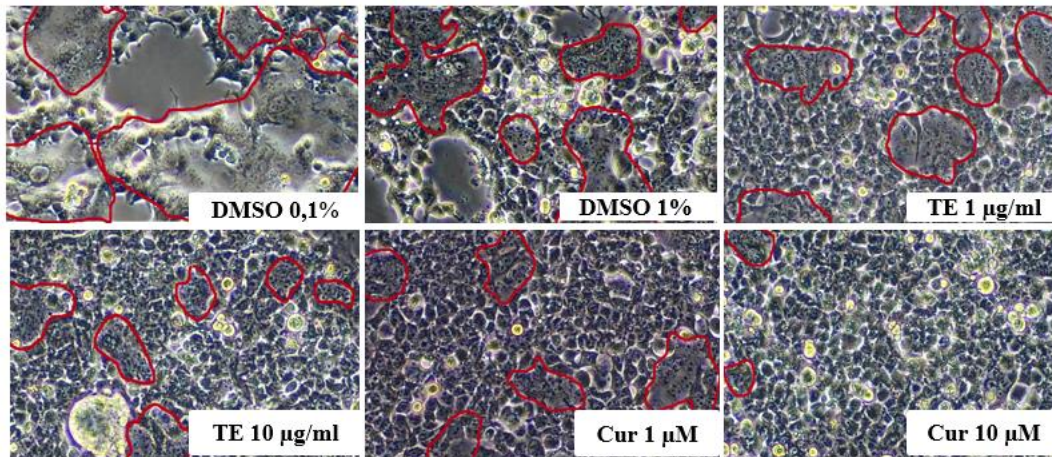
517 expression in 293/hACE2 cells after transduction, before and after selection with antibiotic

518 G418. b. Schematic representation of PSV entry assay in 293/hACE2 stable cells. c. The

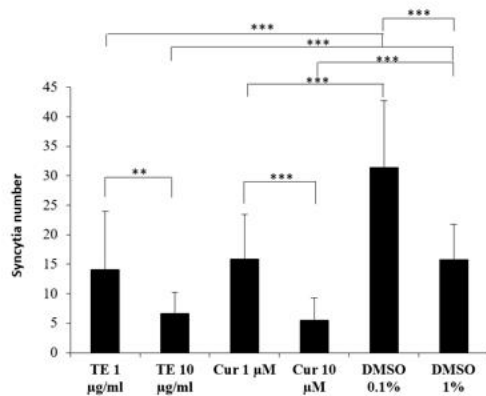
519 representative image shows GFP dots to represent PSV internalization. d. Graph representing

520 quantification of GFP dots (n = 5 microscope fields). P<0.05 = *. NC: nontreated cells.

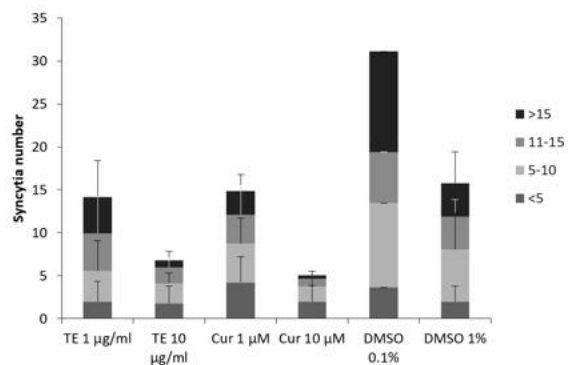
a.



b.



c.



521

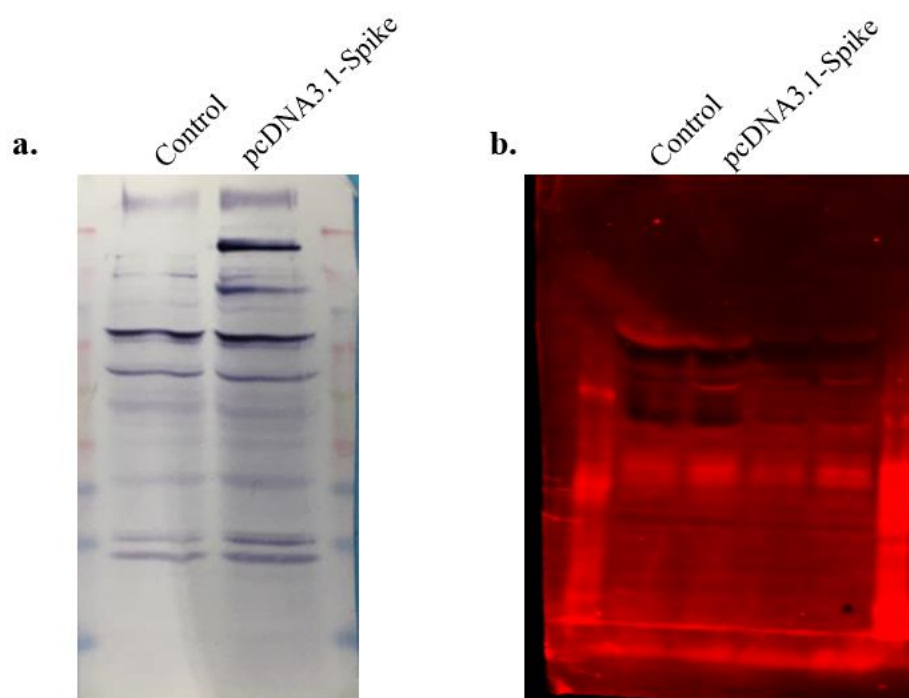
522 **Fig 5. Effect of curcumin and turmeric extract on syncytia formation.** a. Representative
 523 image showing the syncytia formed after curcumin, TE, and DMSO treatment. b. Graph
 524 representing quantification of syncytia number (n = 10 microscopic fields in duplicate). c.
 525 Graph representing quantification of nuclei number per categories of syncytia (n = 10
 526 microscopic fields). Red area: syncytia. P<0.05 = *, P<0.01 = **, P<0.001 = ***, ns = not
 527 significant.

528

529

530

531 **Supplementary**



532

533 **Supplementary Figure 1.** Full membrane image of spike detection by western blot.

534

535